Nuclear Engineering and Technology 51 (2019) 683–691

Contents lists available at ScienceDirect

Nuclear Engineering and Technology

journal homepage: www.elsevier.com/locate/net

Original Article

A novel qEEG measure of teamwork for human error analysis: An EEG hyperscanning study

Kab-Mun Cha*, Hyun-Chul Lee

Korea Atomic Energy Research Institute, 989-111, Daedeok-daero, Yuseong-gu, Daejeon, 34057, South Korea

ARTICLE INFO

Article history:
Received 23 May 2018
Received in revised form
14 October 2018
Accepted 20 November 2018
Available online 21 November 2018

Keywords:
Human error
EEG
Hyperscanning
Bispectral analysis

ABSTRACT

In this paper, we propose a novel method to quantify the neural synchronization between subjects in the collaborative process through electroencephalogram (EEG) hyperscanning. We hypothesized that the neural synchronization in EEGs will increase when the communication of the operators is smooth and the teamwork is better. We quantified the EEG signal for multiple subjects using a representative EEG quantification method, and studied the changes in brain activity occurring during collaboration. The proposed method quantifies neural synchronization between subjects through bispectral analysis. We found that phase synchronization between EEGs of multi subjects increased significantly during the periods of collaborative work. Traditional methods for a human error analysis used a retrospective analysis, and most of them were analyzed for an unspecified majority. However, the proposed method is able to perform the real-time monitoring of human error and can directly analyze and evaluate specific groups.

1. Introduction

Recently, the safety of nuclear technology has become a social issue owing to the accident at the Fukushima nuclear power plant in Japan [1], and it is necessary to have the technical capability to cope with all possible risk factors. Many of the major accidents in the field of nuclear power have been caused by human factors. In the core meltdown of the TMI #2 nuclear power plant in the United States, the problem of an interface insufficiency and procedure implementation of the main control rooms and emergency response facilities [2], the problem of human factors owing to partial automation in the nuclear fuel rods of the French Laurent Nuclear Power Plant, organizational culture and communication problems such as organizational communication and cooperation problems of employees, the JCO critical accidents in Japan, and long-term concealment/false reports of Tokyo Electric Power have been analyzed as human errors [3,4]. Human error means that something has been done that was not desired or intended by a set of rules or an external observer, or that led the task or system outside its acceptable limits [5]. Other factors that cause human error include training and experience, procedures, instrumentation, time Available, complexity, workload/time, pressure/stress, team/crew dynamics, available staffing, human-system interface, environment, accessibility/operability of equipment, need for special tools, etc.

Although the range of factors causing human errors in a nuclear accident is expanding, most of the measures for human error during an incident include a retrospective analysis performed after the occurrence of the incident, and a human reliability analysis (HRA) [6] of only comprehensive situations such as the quantitative probability and safety culture level. As a result, the techniques and standards for human errors against individual human factors, such as the potential adverse mental and physiological condition of the individual when describing human errors in a nuclear accident are still insufficient [3,4]. Therefore, the scope of technical efforts to ergonomically address human error needs to be expanded, or an effective solution must be developed.

One of the fundamental causes of human error is the lack of communication between operators, that is, poor teamwork. In such an environment, there is a high probability that personal mistakes will occur and may lead to an accident. Therefore, a specific and quantitative method for solving this problem is required. In this paper, we propose a real-time teamwork quantification method that is different from the conventional retrospective analysis in order to analyze human errors. Human errors can be reduced by quantifying and managing human factors such as communication

* Corresponding author.
E-mail address: indie486@kaeri.re.kr (K.-M. Cha).

https://doi.org/10.1016/j.net.2018.11.009
1738-5733/

or teamwork.

We hypothesized that the neural synchronization in EEGs will increase when the communication of the operators is smooth and the teamwork is better. We have studied the changes of brain rhythm of multi-subjects through the electroencephalogram (EEG) hyperscanning approach, which has recently attracted attention in the field of neuroscience [7,8]. Hyperscanning refers to the simultaneous recording of hemodynamic or neuro-electrical activity in the brain [9,10]. We quantified the EEG signal for multiple subjects using a representative EEG quantification method, and studied the changes in neural synchronization occurring during collaboration.

Traditional methods for a human error analysis used a retrospective analysis, and most of them were analyzed for an unspecified majority. However, unlike traditional methods, the proposed method can directly analyze and evaluate between individuals or specific groups. In addition, the proposed method can be applied to real-time interaction monitoring systems between operators through quantification of brain activity in a cooperative relationship.

2. Materials and methods

2.1. Subjects

This study was approved by the Korea Atomic Energy Research Institute (Daejeon, Korea). The study included six healthy volunteers (male) over 20 years in age, and the subjects were previously healthy with no abnormal laboratory results.

2.2. EEG recordings

EEG was recorded at two monopolar channels in the frontal lobes (Fp1, Fp2 with the reference electrode in A2 of the international 10–20 system) using a BIO-Single (BioBrain Inc., Daejeon, Korea) with a sampling frequency of 256 Hz. The EEG was continuously recorded before a 'task' (baseline), during a 'task', and after a 'task' (rest). A ninth-order Butterworth filter was used to remove components above 50 Hz from the EEG signals.

2.3. Study design

The experiment was designed to demonstrate the hypothesis that the neural synchronization increases as the subjects perform the same task. We explored neural synchronization by letting two subjects look for the wrong parts of a picture puzzle. The EEGs were recorded simultaneously from two subjects during the experiment. The experiment was carried out in three steps, 'baseline', 'task', and 'rest', which are shown in Fig. 1(a). The 'baseline' and 'rest' sections were conducted with no conversation or movement for 90 s, with their eyes closed. The 'task' section was conducted for 180 s after the 'baseline' section, and a total of six pictures were presented 30 s apart on the screen. As shown in Fig. 1(b), the picture puzzle consists of two same pictures and has a total of 10 different parts. In the 'task' section, the participants were asked to find different parts of the picture with minimal conversation, and a score (0–10) was used to evaluate the performance of task in each picture.

2.4. EEG hyperscanning

One of the most important features of human behavior is interpersonal collaboration; however, owing to the technical limitations of brain imaging techniques that simultaneously track the brains of multi-subjects during collaborative work, the neurological characteristics explaining this part have been little known. However, research on EEG such as fMRI and EEG is ongoing. The simultaneous recording and analysis of brain hemodynamic or neuro-electrical activity on multiple subjects is called 'Hyperscanning' [7–10]. Hyperscanning was proposed as a tool for social interaction research in fMRI [11], and then applied to the neuroelectrical field to conduct studies on decision making and attention [12,13].

The introduction of the EEG hyperscanning approach and the portable EEG recording system provided ecological experiment settings that allow people to interact naturally [13,14]. EEG-based hyper-connectivity studies between subjects participating in cooperating tasks showed validity in predicting cooperative behaviors [7–10]. In this paper, we propose a novel method to quantify the neural synchronization between subjects in the collaborative process through EEG hyperscanning.

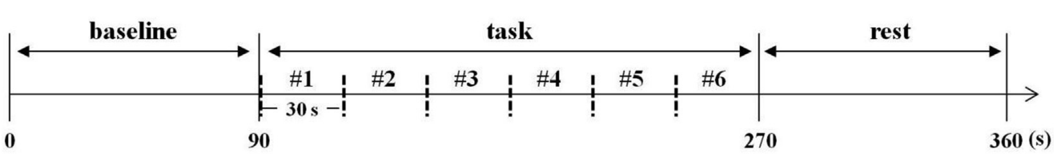

(a)

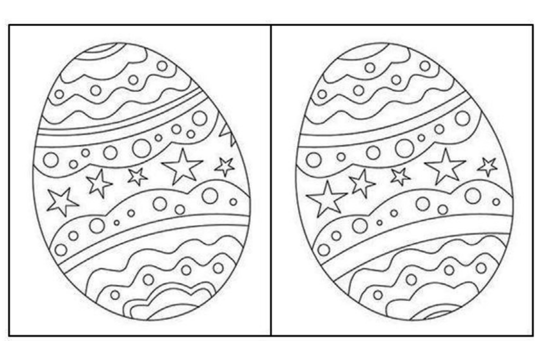

(b)

Fig. 1. The study design. (a) Timeline of the experiment, (b) an example of the picture puzzle.

2.5. Conventional methods

We compared three quantitative EEG (qEEG) methods to confirm the changes in neural activities of multiple subjects.

2.5.1. Mutual information

Mutual information measuring the information shared by both the X and Y signals [15], is generally defined as follows:

$$MI(X;Y)=\sum_{x,y}p(x,y)\ln\frac{p(x,y)}{p(x)p(y)} \tag{1}$$

where $p(x,y)$ is the joint probability distribution function of X and Y. Here, $p(x)$ and $p(y)$ are the marginal probability distribution function of X and Y, respectively. This equation can be expressed as a sum of the Shannon entropies, namely,

$$MI(X;Y)=H(X)+H(Y)-H(X,Y) \tag{2}$$

and when defining the EEG signals obtained from two different regions of the brain as X and Y, (2) can be used to quantify the degree of information shared by the two regions. In addition, by applying this principle to multiple subjects, the amount of information shared among multiple subjects can be confirmed.

2.5.2. Transfer entropy

Transfer entropy is the measurement used to quantify the effect of information obtained from Y (y_n) signal at a specific time n on the X (x_{n+1}) signal at a future time [16]. When defining each probability distribution for x_n and y_n as $p(x)$ and $p(y)$, respectively, TE from Y to X is defined as follows:

$$T_{Y\rightarrow X}=\sum_{x,y}p\left(x_{n+1},x_n^{(k)},y_n^{(k)}\right)\ln\frac{p\left(x_{n+1}\middle|x_n^{(k)},y_n^{(k)}\right)}{p\left(x_{n+1}\middle|x_n^{(k)}\right)} \tag{3}$$

where $x_n^{(k)}$ denotes $x_{n-(k-1)},x_{n-2(k-1)},\dots,x_{n-d(k-1)}$, in which d is the embedding dimension and k is the embedding delay. We applied the uniform embedding scheme [17] to evaluate TE, and we fixed the embedding dimension and the embedding delay at 1 for computational reasons [16]. TE in Eq. (3) can be obtained as follows:

$$\begin{aligned}T_{B\rightarrow A}&=H(A_{n+1}|A_n)-H(A_{n+1}|A_n,B_n)\\&=H(A_{n+1}|A_n)-H(A_n)\ -\{H(A_{n+1},A_n,B_n)-H(A_n,B_n)\}\end{aligned} \tag{4}$$

where A is a target group and B is a source group. For a multivariate random vector, A, assuming the Gaussian p.d.f. in Ref. [18], the Shannon entropy [15] can be calculated as follows:

$$H(A)=\frac{1}{2}\ln(2\pi e)^k|\Sigma_A| \tag{5}$$

where k is the number of random variables, Σ_A is the covariance matrix of A, and $|\cdot|$ denotes the matrix determinant.

2.5.3. Partial directed coherence

Recently, hyperscanning studies using PDC have been conducted [7,8]. Partial directed coherence (PDC) is a Granger-causality [19] based spectral estimator providing the directed influences between the pair of signals in a multivariate dataset [20].

When the n-dimensional time series signal is $x(t)=(x_1(t),\ \dots,\ x_n(t))$ the vector autoregressive model (VAR) for x can be expressed as follows:

$$X(t)=\sum_{r=1}^{p}a(r)X(t-r)+\varepsilon(t) \tag{6}$$

where $a_{ij}(r)$ indicates how the current value of x_i linearly depends on the past value of x_j. It is the PDC that introduces this concept into the frequency domain.

$$A(\omega)=I-\sum_{r=1}^{p}a(r)e^{-i\omega r} \tag{7}$$

Equation (7) above represents the difference between the n -dimensional identity matrix I and the Fourier transform of the coefficient sequence. Here, the PDC is defined as follows:

$$\left|\pi_{i-j}(\omega)\right|=\frac{\left|A_{ij}(\omega)\right|}{\sqrt{\sum_k\left|A_{kj}(\omega)\right|^2}} \tag{8}$$

PDC means the linear effect of x_j on x_i at frequency ω, and can be used to confirm the connectivity of the EEG signals to multiple subjects.

2.6. Proposed method

The proposed method quantifies neural synchronization between subjects through bispectral analysis. A bispectral analysis had been carried out for EEG signal monitoring, and is used to study nonlinear relationships in the recorded EEG from multiple electrodes, an evaluation of the anesthetic effects, and EEG changes under various physiological conditions [21,22]. These studies have shown that a bispectral analysis can extract useful information that cannot be obtained through a power spectral analysis. The bispectrum approach is a method of measuring the degree of phase coupling between two spectral components contained in a signal [22,23]. Unlike the PDC, which only uses the power spectrum, the phase information is not ignored. The bispectrum magnitude is defined as

$$B_{fL-fH\ Hz}\left(f_i,\ f_j\right)=\left|\sum_l X_l(f_i)X_l\left(f_j\right)X_l^*\left(f_i+f_j\right)\right|,\qquad f_i\ ,\ f_j\in\ [f_L\ ,\ f_H] \tag{9}$$

where X_l denotes the spectral component of the l th epoch, and X_l^* its conjugate. The power spectrum is a function for a single frequency variable (f_i), but the bispectrum is a function for two frequency variables (f_i,f_j).

As an example of a bispectrum [22], consider the case of a simple nonlinear system whose output $\gamma(k)$ is the square of its input $x(k)$:

$$\gamma(k)=x^2(k) \tag{10}$$

If the input signal is the sum of two sinusoids of frequencies f_1 and f_2, and random, independent phase angles θ_1 and θ_2, respectively, the output signal is

$$\begin{aligned}x(k)&=\cos(f_1k+\theta_1)+\cos(f_2k+\theta_2)\\ \gamma(k)&=1+\cos((f_1+f_2)k+(\theta_1+\theta_2))+\cos((f_1-f_2)k+(\theta_1-\theta_2))\\&\quad+{}^1\!/\!_2\cos(2f_1k+2\theta_1)+{}^1\!/\!_2\cos(2f_2k+2\theta_2)\end{aligned} \tag{11}$$

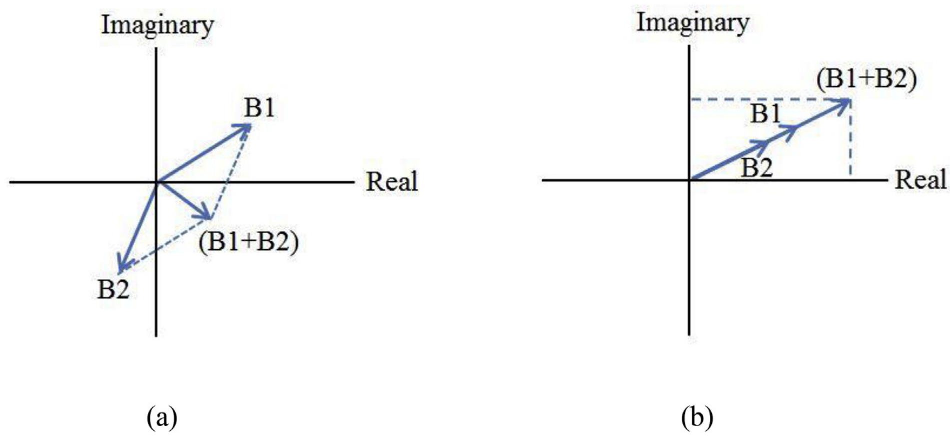

Fig. 2. The sum of the spectral values for the two bispectrum: (a) Bispectrum of signals made up of only independent fundamentals with random phases, (b) bispectrums of signals made up of fundamentals with nonrandom (coupled) phase components.

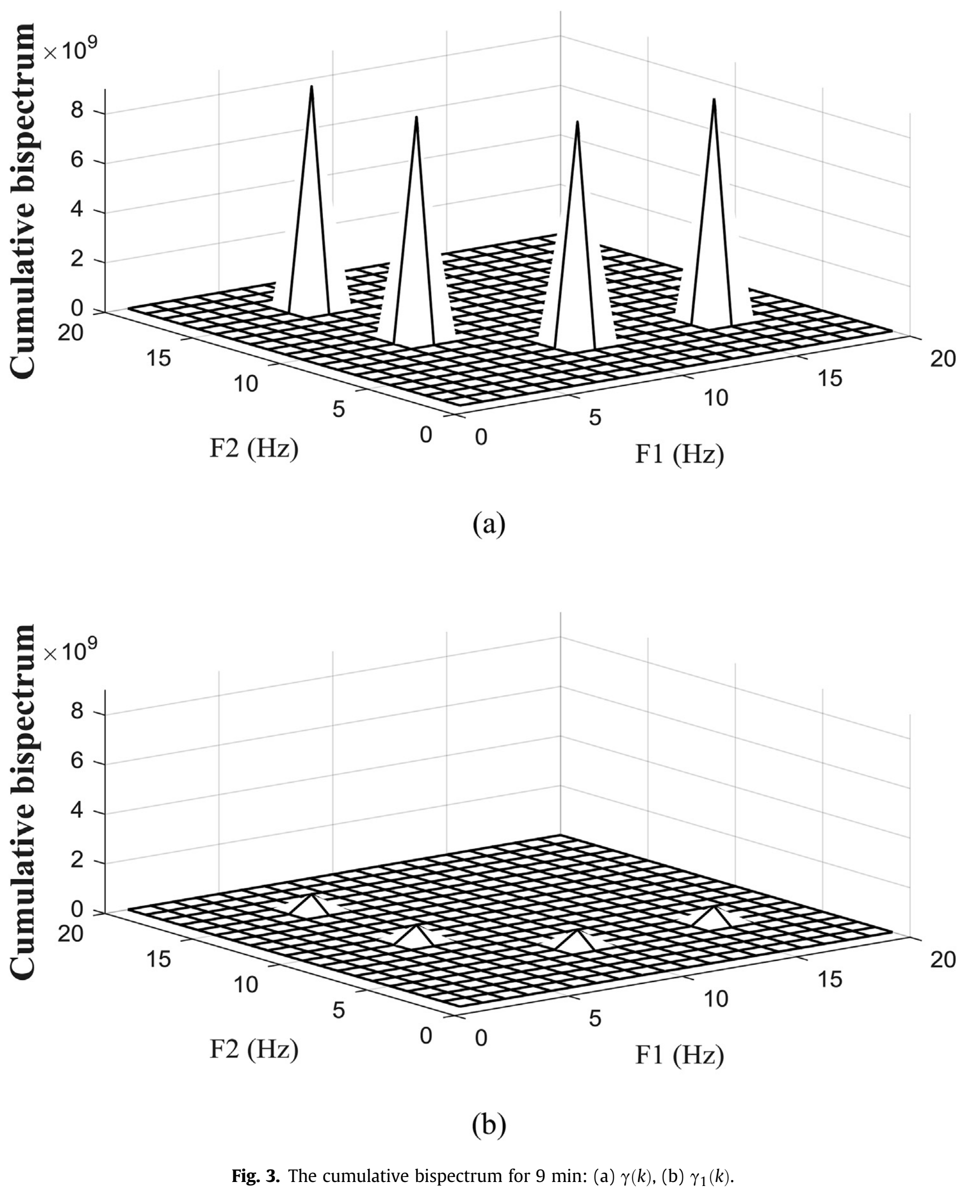

Fig. 3. The cumulative bispectrum for 9 min: (a) $\gamma(k)$, (b) $\gamma_1(k)$.

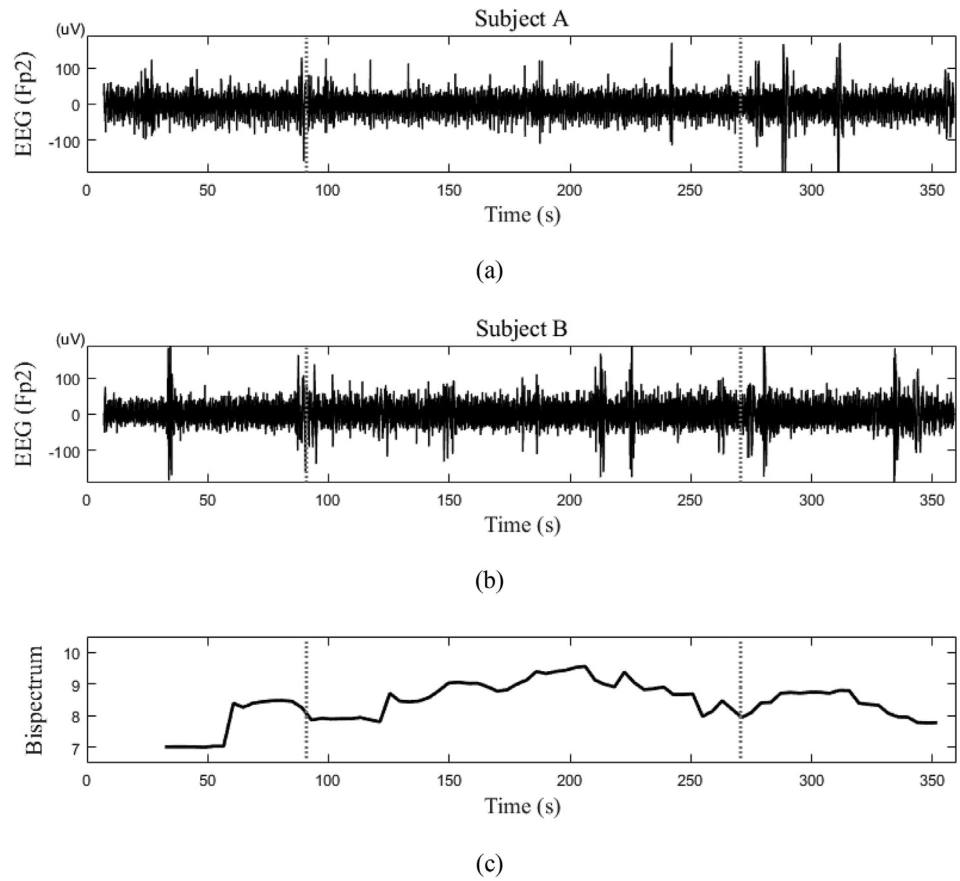

Fig. 4. Example of bispectrum using EEG dataset (the two vertical dashed lines indicate the start and end of the task): (a) raw EEG signal from prefrontal lobe (Fp2) of subject A for 6 min, (b) Raw EEG signal from prefrontal lobe (Fp2) of subject B, (c) time evolution of bispectrum.

where θ_1 and θ_2 are random and independent. The frequency components of the resultant signal $\gamma(k)$, $f_1+f_2, f_1-f_2, 2f_1$ and $2f_2$ are dependent on f_1 and f_2. Then, the signal $\gamma_1(k)$ with the same power spectrum as $\gamma(k)$ in equation (11) can be constructed by adding together independent frequency components with frequencies $f_1+f_2, f_1-f_2, 2f_1$ and $2f_2$.

$$\begin{aligned}\gamma_1(k) = 1 + \cos(f_a k + \theta_a) + \cos(f_b k + \theta_b) \\ + {}^1\!/\!2\cos(f_c k + \theta_c) + {}^1\!/\!2\cos(f_d k + \theta_d)\end{aligned} \tag{12}$$

where $f_a = f_1+f_2, f_b = f_1-f_2, f_c = 2f_1, f_d = 2f_2$, and θ_a, θ_b, θ_c, and θ_d are random and independent. The signal $\gamma_1(k)$ has a completely different phase structure than the output signal $\gamma(k)$. Yet, its power spectrum is identical to that of the signal $\gamma(k)$. In the case of a signal made up of only independent fundamentals with random phases, $\gamma_1(k)$, cumulative bispectrum from successive epochs will cause components of the same frequency, but having random phase angles, to cancel each other and thus sum to small value (Fig. 2a). However, nonrandom (coupled) phase components will sum to big non-zero value (Fig. 2b).

The cumulative bispectrum of these two signals $\gamma(k)$ and $\gamma_1(k)$ is shown in Fig. 3. The frequency components f_1 and f_2 was set to 5 Hz and 11 Hz, respectively. The phase angles θ_1 and θ_2 of the signal $\gamma(k)$ were set to 0, and the phase angle θ_a, θ_b, θ_c, and θ_d of the signal $\gamma_1(k)$ were set to random. The signals $\gamma(k)$ and $\gamma_1(k)$ were equally divided into 4 s intervals to calculate the bispectrum. The bispectrum of $\gamma(k)$ and $\gamma_1(k)$ was cumulative for 9 min (135 epochs).

Fig. 4 shows an example of a bispectrum for an EEG dataset from multiple subjects. Fig. 4(a) and (b) show the EEG signal of the prefrontal lobe (Fp2) from two subjects, and Fig. 4(c) shows the time evolution of bispectrum; the two vertical dashed lines indicate the time points of the start and end of the task. For the data analysis, the EEG signal was equally divided into 4 s epochs. To compute the bispectrum, the EEG signal is first divided into a series of epochs adjusted to a zero mean value in order to exclude from analysis any signal offset arising from electrode half-cell potentials [22].

According to Nikias and Raghuveer, an overlapping method is effective in increasing the total number of epochs in the restricted sampling records [24]. Bispectrum was calculated by using the EEG data for 32 s at a 4-s interval. Then, the bispectrum of EEGs from two subjects was calculated by applying equation (11).

In the figure, the bispectrum shows higher values than 'baseline' or 'rest' section in the 'task' section. This result means that phase coupling with two subjects increases in collaboration.

3. Results

The efficacy of the proposed method was confirmed in a total of six subjects. To demonstrate the efficacy of conventional methods and the proposed method, all methods were applied to the EEG signal obtained during a period of 6 min, which included three sections (baseline, task, and rest). The EEG signal was equally divided into 4 s epochs and the sampling rate is 256 Hz. To prevent the spectrum distortion owing to the Discrete Fourier Transform (DFT) procedure, the Blackman window was applied to each epoch, and the Fast Fourier Transform (FFT) was used to obtain the spectral components.

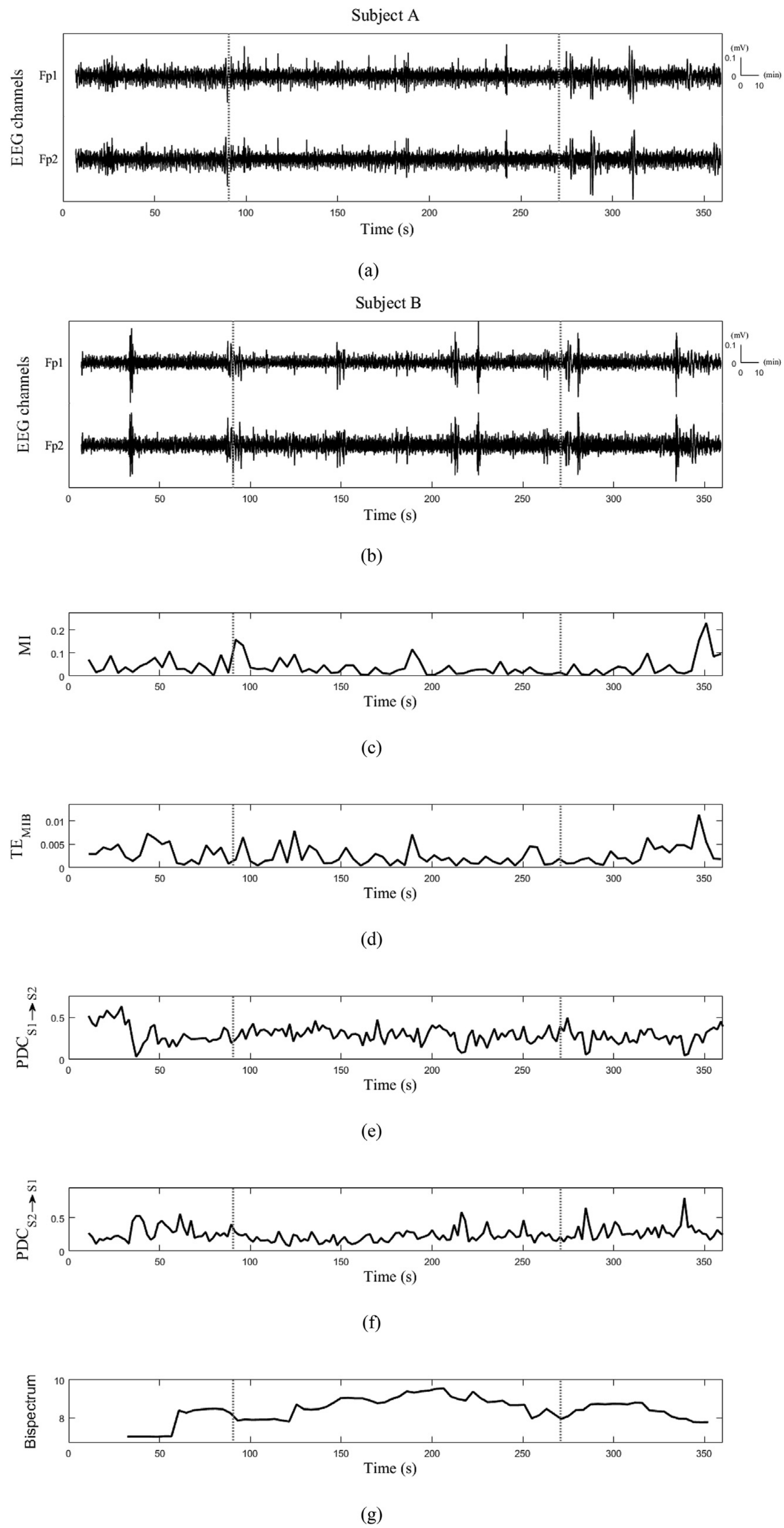

Fig. 5. Example of conventional methods and proposed method using EEG data (the two vertical dashed lines indicate the start and the end of the task): (a) raw EEGs (Fp1 and Fp2) of Subject A for 6 min, (b) raw EEGs (Fp1 and Fp2) of Subject B, (c) mutual information between subject A and subject B, (d) transfer entropy with MIB, (e) partial directed coherence from subject A to subject B, (f) partial directed coherence from subject B to subject A, and (g) bispectrum between subject A and subject B.

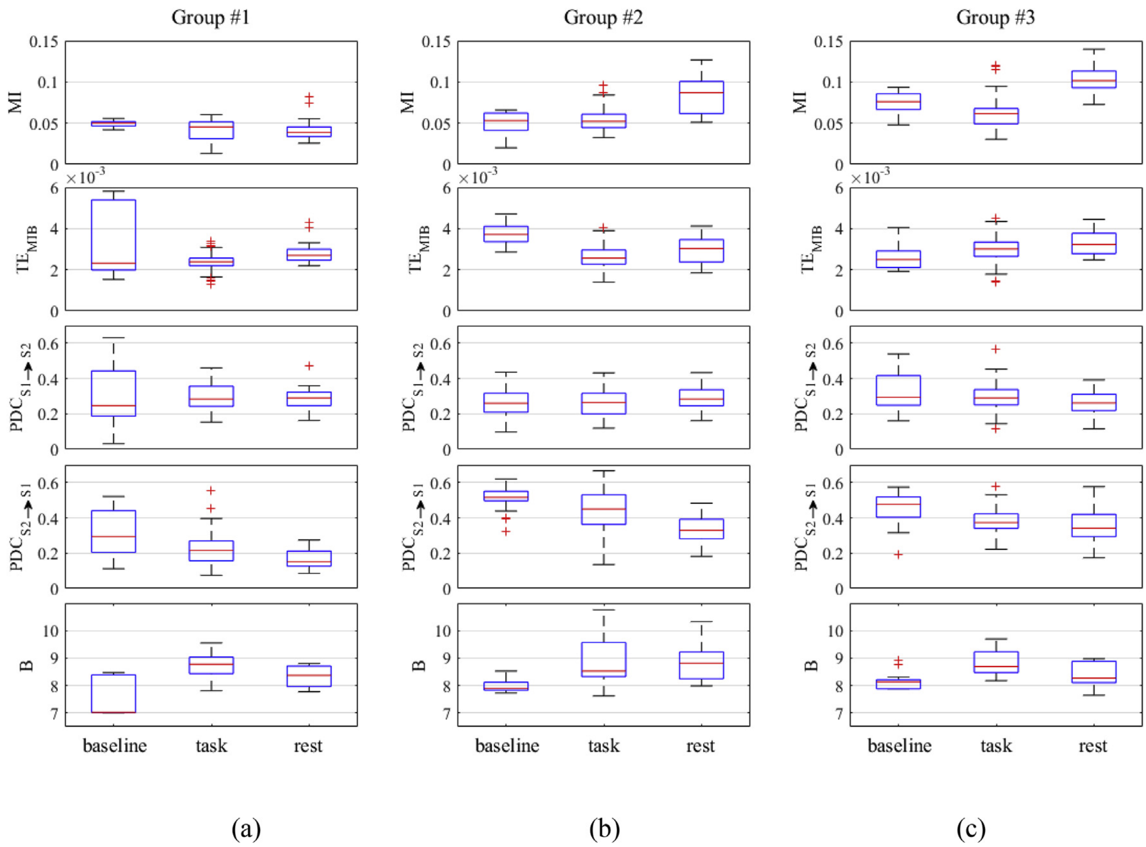

Fig. 6. Boxplots of the conventional and proposed methods for three groups. The middle line is the median value: (a) group #1, (b) group #2, and (c) group #3.

Fig. 5 shows the results of the proposed and conventional methods such as mutual information (MI), transfer entropy (TE), and partial directed coherence (PDC). The EEG signal derived from four channels, Fp1 and Fp2 of each subject, was used for calculating the conventional methods, and two EEG channels (Fp2 of each subject) were used for the proposed method. The recording intervals were divided into three sections according to the subject's collaboration: section A is the baseline phase without an interaction between subjects, section B is the task phase with collaboration between subjects, and section C is the rest phase with their eyes closed.

Fig. 5(a) and (b) show EEG channels for a total of 6 min before and after a collaboration 'task'; the two vertical dashed lines indicate the time points of the start of the task section and end of the task, respectively. Fig. 5(c) shows the results of mutual information for the EEG signals of the prefrontal lobe (Fp1 and Fp2) from subject A and subject B. The figure does not reflect the change well, as there is little change in the figure thereafter. Fig. 5(d) shows the results of transfer entropy with minimum information bipartition (MIB) [25] for the EEG signals of the prefrontal lobe (Fp1 and Fp2) from subject A and subject B, and the time delay of TE is 7.8 ms. The MIB divides channels into two subgroups such that they have the minimum information flow. Then, among these partitions, the partition that has the greatest amount of information is selected [25,26]. Although this method cannot avoid the directed or mediated influences between channels, it is suitable for reflecting the functional integration and segregation of the EEGs. Fig. 5(e) and (f) show the results of partial directed coherence from prefrontal lobe (Fp2) of subject A to the prefrontal lobe (Fp2) of subject B and vice versa, respectively. Fig. 5(g) shows the results of bispectrum for the EEG signals of the prefrontal lobe (Fp2) from subject A and the prefrontal lobe (Fp2) from subject B. In this figure, bispectrum shows the remarkable trend of the increased figure at the task section and the decreased figure after a task, clearly reflecting the neural changes.

Fig. 6 shows the results of the conventional and proposed methods for three groups (six subjects). Boxplots of all methods at three sections (baseline, task, and rest) are expressed with median values and quartiles (25–75%) for each section, respectively. This result shows that the bispectrum value increases

Table 1
Statistics of all methods for three sections (mean(std)).

Meaures	Group #1			Group #2			Group #3		
	baseline	task	rest	baseline	task	rest	baseline	task	rest
MI ($\times 10^1$)	0.49(0.04)	0.41(0.013)	0.43(0.15)	0.51(0.14)	0.56(0.16)	0.84(0.23)	0.76(0.13)	0.61(0.20)	1.03(0.16)
TEMIB ($\times 10^2$)	0.32(0.17)	0.23(0.05)	0.28(0.06)	0.37(0.06)	0.26(0.07)	0.30(0.07)	0.26(0.06)	0.30(0.07)	0.33(0.05)
PDC (S1 $\rightarrow$ S2)	0.31(0.17)	0.30(0.07)	0.29(0.07)	0.26(0.08)	0.26(0.09)	0.29(0.07)	0.32(0.10)	0.30(0.09)	0.26(0.07)
PDC (S2 $\rightarrow$ S1)	0.32(0.14)	0.22(0.09)	0.17(0.06)	0.51(0.07)	0.44(0.12)	0.36(0.08)	0.46(0.09)	0.38(0.08)	0.36(0.11)
Bispectrum	7.59(0.71)	8.69(0.51)	8.36(0.36)	8.01(0.26)	8.88(0.88)	8.84(0.06)	8.22(0.31)	8.83(0.44)	8.43(0.42)

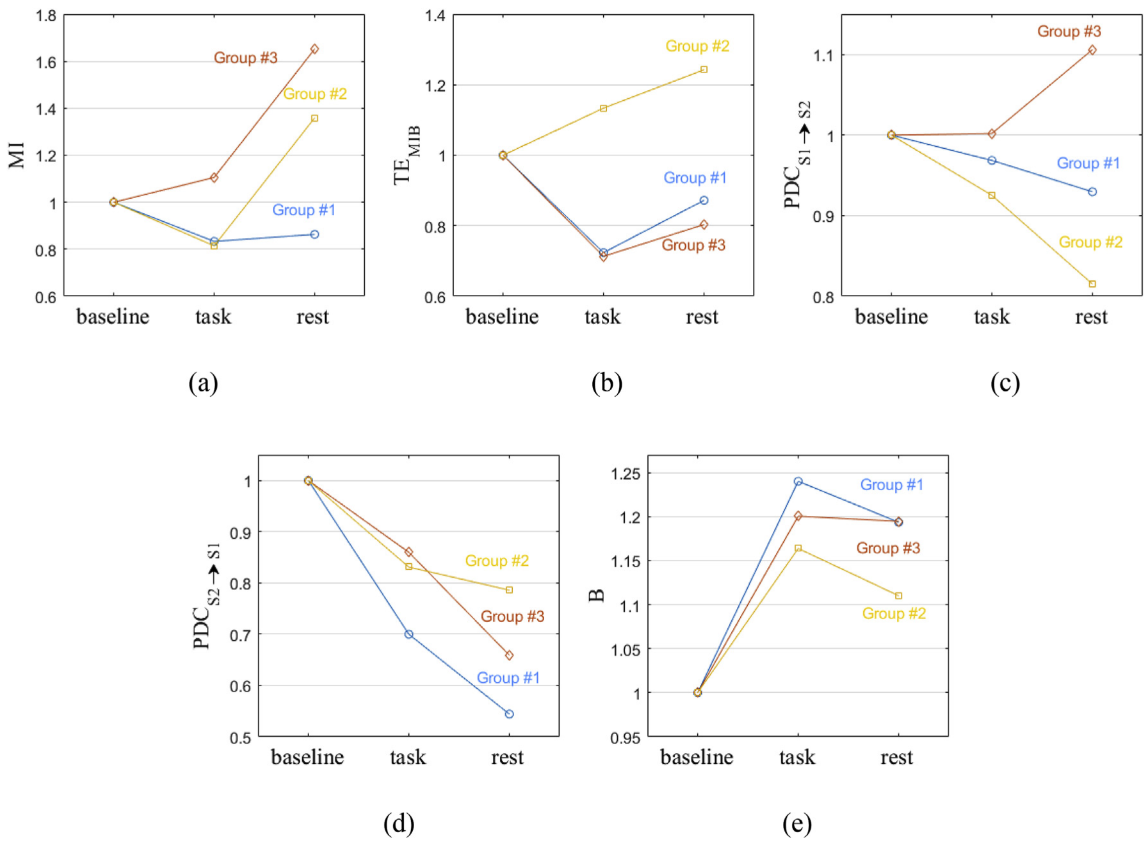

Fig. 7. The normalized and averaged results of three groups: (a) MI, (b) TE with MIB, (c) PDC (S1→S2), (d) PDC (S2→S1), and (e) Bispectrum.

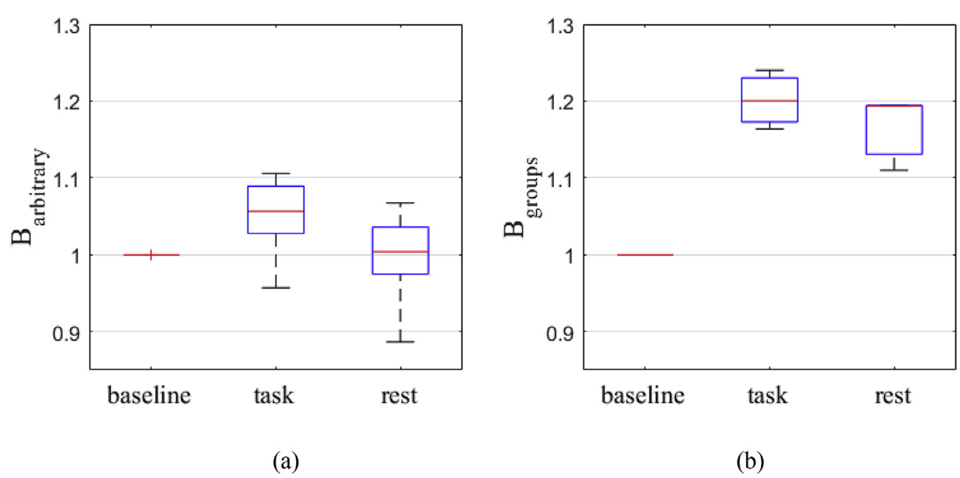

Fig. 8. Verification of bispectral analysis results (the red line indicates the median value): (a) bispectrum for arbitrary combinations of six subjects (μ of the task section is 1.028 and μ of the rest section is 1.017), and (b) bispectrum for three groups (μ of the task section is 1.201 and μ of the rest section is 1.166). (For interpretation of the references to colour in this figure legend, the reader is referred to the Web version of this article.)

during collaboration. The statistics in each section are shown in Table 1.

To quantitatively compare various methods and remove subject dependency, the results of the measures were normalized with the mean value of the baseline section for each subject, which are shown in Fig. 7. In the figure, except for the bispectrum, no noticeable change is observed. In the bispectral analysis, the tendency for the bispectrum value to increase in the task section is clearly shown, and it can be seen that it increased by more than 20% on average compared with the baseline.

To verify whether the results of the bispectral analysis is due to collaboration, we confirmed the bispectrum results for the arbitrary combinations (12 combinations) of six subjects excluding the pairs that participated in the experimental series. As shown in Fig. 8, the bispectrum results for the arbitrary combinations does not reflect the change in the neural synchronization.

4. Conclusions

In this paper, to analyze and prevent human error, which is one of the main causes of a nuclear accident, we studied a quantitative index for evaluating the activities related to mutual interaction and teamwork among the operators. We used 'EEG hyperscanning' to test the neural synchronization of multi-subjects and applied conventional methods and the proposed method used for EEG quantification. A collaborative experiment was performed to verify the hypothesis that the brain rhythm in the 'rest' phase, where there is no communication between subjects, and the brain rhythm in the 'task' phase, which is collaborative, will be different.

The absence of neural synchronization does not mean that some error has been committed. To obtain such evidence, we may have to design experiments to register human error. It is not easy to derive a direct relationship between human error and neural synchronization. However, we confirmed the neural synchronization during cooperative work using a 'bispectral analysis' and confirmed the possibility of evaluation as an index for a human error analysis. In the present stage, the proposed method can be used to scan for abnormalities of the operators before working, and it is expected that the proposed method will be possible to monitor the status of the operators in real time through the development of a miniaturized and wireless EEG sensor. However, to increase the reliability as an index, experiments of various brain regions and further supplementation of performance are required.

Competing Interests

Conflict of interest

None.

Acknowledgements

This research was supported by Nuclear R&D Program through the National Research Foundation of Korea funded by the Ministry of Science and ICT (Grant No. 2017M2A8A4017947).

References

[1] K. Hirose, 2011 Fukushima Dai-ichi nuclear power plant accident: summary of regional radioactive deposition monitoring results, J. Environ. Radioact. 111 (2012) 13–17.
[2] P. Le Bot, Human reliability data, human error and accident models—illustration through the Three Mile Island accident analysis", Reliab. Eng. Syst. Saf. 83 (2) (2004) 153–167.
[3] T.I. Jang, et al., State of the art report for the development of countermeasures against human errors caused by individual factors in Npps, KAERI/AR 959 (2012).
[4] H.C. Lee, et al., Development of Human Error Countermeasures for Nuclear Safety, 4163, KAERI/RR, 2016.
[5] J.W. Senders, N.P. Moray, Human Error: Cause, Prediction, and Reduction, 25, Lawrence Erlbaum Associates, 1991. ISBN 0-89859-598-3.
[6] A.D. Swain, H.E. Guttmann, Handbook of Human-reliability Analysis with Emphasis on Nuclear Power Plant Applications. Final Report, Sandia National Labs., Albuquerque, NM (USA), 1983.
[7] J. Toppi, G. Borghini, M. Petti, E.J. He, G.V. De, B. He, L. Astolfi, F. Babiloni, Investigating cooperative behavior in ecological settings: an EEG hyperscanning study, PloS One 11 (4) (2016).
[8] A.P. Burgess, On the interpretation of synchronization in EEG hyperscanning studies: a cautionary note, Front. Hum. Neurosci. 7 (2013) 881.
[9] F. Babiloni, L. Astolfi, Social neuroscience and hyperscanning techniques: past, present and future, Neurosci. Biobehav. Rev. 44 (2014) 76–93.
[10] L. Astolfi, J. Toppi, F. Fallani, G. Vecchiato, S. Salinari, D. Mattia, F. Cincotti, F. Babiloni, Neuroelectrical hyperscanning measures simultaneous brain activity in humans, Brain Topogr. 23 (3) (2010) 243–256.
[11] P.R. Montague, G.S. Berns, J.D. Cohen, S.M. McClure, G. Pagnoni, M. Dhamala, M.C. Wiest, I. Karpov, R.D. King, M. Apple, R.E. Fisher, Hyperscanning: simultaneous fMRI during linked social interactions, Neuroimage 16 (2002) 1159–1164.
[12] H. Tang, X. Mai, S. Wang, C. Zhu, F. Krueger, C. Liu, Interpersonal brain synchronization in the right temporo-parietal junction during face-to-face economic exchange, Soc. Cognit. Affect Neurosci. 11 (1) (2015) 23–32.
[13] D.V. Fallani, et al., "Defecting or not defecting: how to "read" human behavior during cooperative games by EEG measurements", PloS One 5 (12) (2010) e14187.
[14] G. Dumas, J. Nadel, R. Soussignan, J. Martinerie, L. Garnero, Inter-brain synchronization during social interaction, PloS One 5 (8) (2010) e12166.
[15] C.E. Shannon, W. Weaver, The Mathematical Theory of Information, 1949.
[16] T. Schreiber, Measuring information transfer, Phys. Rev. Lett. 85 (2) (2000) 461–464.
[17] D. Marinazzo, O. Gosseries, M. Boly, D. Ledoux, M. Rosanova, M. Massimini, Q. Noirhomme, S. Laureys, Directed information transfer in scalp electroencephalographic recordings: insights on disorders of consciousness, Clin. EEG Neurosci. 45 (1) (2014) 33–39.
[18] S. Johansen, "Estimation and hypothesis testing of cointegration vectors in Gaussian vector autoregressive models", *Econometrica*, Journal of the Econometric Society 59 (6) (1991) 1551–1580.
[19] C.W.J. Granger, Investigating causal relations by econometric models and cross-spectral methods, *Econometrica*: Journal of the Econometric Society (1969c) 424–438.
[20] L.A. Baccalá, K. Sameshima, Partial directed coherence: a new concept in neural structure determination, Biol. Cybern. 84 (6) (2001) 463–474.
[21] J.W. Johansen, P.S. Sebel, Development and clinical application of electroencephalographic bispectrum monitoring, Anesthesiology 93 (5) (2000) 1336–1344.
[22] J.C. Sigl, N.G. Chamoun, An introduction to bispectral analysis for the electroencephalogram, J. Clin. Monit. 10 (6) (1994) 392–404.
[23] S. Hagihira, M. Takashina, T. Mori, T. Mashimo, I. Yoshiya, Practical issues in bispectral analysis of electroencephalographic signals, Anesth. Analg. 93 (4) (2001) 966–970.
[24] C.L. Nikias, M.R. Raghuveer, Bispectrum estimation: a digital signal processing framework, Proc. IEEE 75 (7) (1987) 869–897.
[25] G. Tononi, O. Sporns, Measuring information integration, BMC Neurosci. 4 (31) (2003).
[26] G. Tononi, An information integration theory consciousness, BMC Neurosci. 5 (1) (2004).